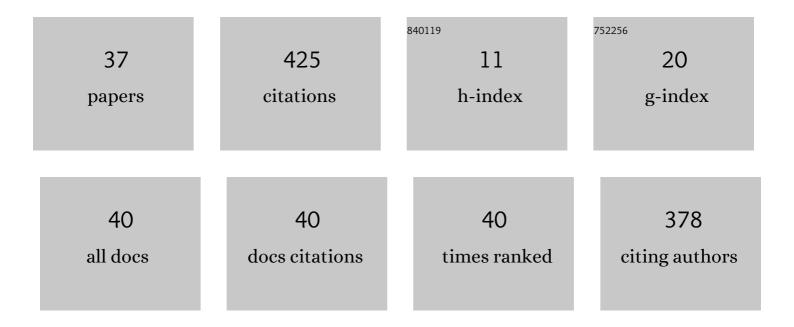
Hyosim Kim

List of Publications by Year in descending order

Source: https://exaly.com/author-pdf/5971668/publications.pdf Version: 2024-02-01



HVOSIM KIM

#	Article	IF	CITATIONS
1	Radiation response of alloy T91 at damage levels up to 1000 peak dpa. Journal of Nuclear Materials, 2016, 482, 257-265.	1.3	59
2	Beam-contamination-induced compositional alteration and its neutron-atypical consequences in ion simulation of neutron-induced void swelling. Materials Research Letters, 2017, 5, 478-485.	4.1	45
3	Standardization of accelerator irradiation procedures for simulation of neutron induced damage in reactor structural materials. Nuclear Instruments & Methods in Physics Research B, 2017, 409, 251-254.	0.6	34
4	Radiation response of Ti2AlC MAX phase coated Zircaloy-4 for accident tolerant fuel cladding. Journal of Nuclear Materials, 2019, 523, 26-32.	1.3	33
5	Radiation instability of equal channel angular extruded T91 at ultra-high damage levels. Acta Materialia, 2017, 132, 395-404.	3.8	31
6	Interface reactions and mechanical properties of FeCrAl-coated Zircaloy-4. Journal of Nuclear Materials, 2019, 519, 57-63.	1.3	26
7	Swelling resistance of advanced austenitic alloy A709 and its comparison with 316 stainless steel at high damage levels. Journal of Nuclear Materials, 2019, 527, 151818.	1.3	23
8	Ni coating on 316L stainless steel using cage plasma treatment: Feasibility and swelling studies. Journal of Nuclear Materials, 2020, 540, 152385.	1.3	18
9	Impact of composition modification induced by ion beam Coulomb-drag effects on the nanoindentation hardness of HT9. Nuclear Instruments & Methods in Physics Research B, 2019, 444, 68-73.	0.6	14
10	Radiation response of oxide-dispersion-strengthened alloy MA956 after self-ion irradiation. Nuclear Instruments & Methods in Physics Research B, 2017, 409, 259-263.	0.6	13
11	Irradiation-induced swelling of pure chromium with 5 MeV Fe ions in the temperature range 450–650°C. Journal of Nuclear Materials, 2021, 543, 152585.	1.3	12
12	Comparison of void swelling of ferritic-martensitic and ferritic HT9 alloys after high-dose self-ion irradiation. Materials Characterization, 2021, 173, 110908.	1.9	11
13	Dispersoid stability in ion irradiated oxide-dispersion-strengthened alloy. Journal of Nuclear Materials, 2018, 509, 504-512.	1.3	10
14	Radiation response of a Fe–20Cr–25Ni austenitic stainless steel under Fe2+ irradiation at 500°C. Materialia, 2020, 9, 100542.	1.3	8
15	Sizing up mechanical testing: Comparison of microscale and mesoscale mechanical testing techniques on a FeCrAl welded tube. Journal of Materials Research, 2020, 35, 2817-2830.	1.2	8
16	Nitrogen ion implantation into pure iron for formation of surface nitride layer. Nuclear Instruments & Methods in Physics Research B, 2019, 451, 10-13.	0.6	7
17	Radiation-Enhanced Anion Transport in Hematite. Chemistry of Materials, 2021, 33, 2307-2318.	3.2	7
18	Void swelling of conventional and composition engineered HT9 alloys after high-dose self-ion irradiation. Journal of Nuclear Materials, 2022, 560, 153492.	1.3	7

Нуозім Кім

#	Article	IF	CITATIONS
19	A pathway to synthesizing single-crystal Fe and FeCr films. Surface and Coatings Technology, 2020, 403, 126346.	2.2	6
20	Radiation response of FeCrAl-coated Zircaloy-4. Journal of Nuclear Materials, 2020, 536, 152175.	1.3	6
21	Helium retention, bubble superlattice formation and surface blistering in helium-irradiated tungsten. Journal of Nuclear Materials, 2021, 545, 152722.	1.3	6
22	Microstructural and micro-mechanical analysis of 14YWT nanostructured Ferritic alloy after varying thermo-mechanical processing paths into tubing. Materials Characterization, 2021, 171, 110744.	1.9	5
23	Radiation Enhanced Anion Diffusion in Chromia. Journal of Physical Chemistry C, 2021, 125, 27820-27827.	1.5	5
24	Effect of Helium on Dispersoid Evolution under Self-Ion Irradiation in A Dual-Phase 12Cr Oxide-Dispersion-Strengthened Alloy. Materials, 2019, 12, 3343.	1.3	4
25	The Effect of Internal Free Surfaces on Void Swelling of Irradiated Pure Iron Containing Subsurface Trenches. Crystals, 2019, 9, 252.	1.0	4
26	ZrN Phase Formation, Hardening and Nitrogen Diffusion Kinetics in Plasma Nitrided Zircaloy-4. Materials, 2021, 14, 3572.	1.3	4
27	Stable, Ductile and Strong Ultrafine HT-9 Steels via Large Strain Machining. Nanomaterials, 2021, 11, 2538.	1.9	3
28	Carbon Contamination, Its Consequences and Its Mitigation in Ion-Simulation of Neutron-Induced Swelling of Structural Metals. Minerals, Metals and Materials Series, 2018, , 681-693.	0.3	2
29	Ion cutting of amorphous metals by using helium ion implantation. Nuclear Instruments & Methods in Physics Research B, 2019, 451, 1-5.	0.6	2
30	Oxide dispersoid coherency of a ferritic-martensitic 12Cr oxide-dispersion-strengthened alloy under self-ion irradiation. Journal of Nuclear Materials, 2021, 544, 152671.	1.3	2
31	Carbon Contamination, Its Consequences and Its Mitigation in Ion-Simulation of Neutron-Induced Swelling of Structural Metals. Minerals, Metals and Materials Series, 2019, , 681-693.	0.3	2
32	Demonstration of a High-Throughput Tensile Testing Technique Using Femtosecond Laser-Fabricated Tensile Bars in AISI 316 and Additively Manufactured Grade 91 Steel. Jom, 2021, 73, 4240-4247.	0.9	2
33	Continuous Monitoring of Pure Fe Corrosion in Lead-Bismuth Eutectic Under Irradiation with Proton-Induced X-ray Emission Spectroscopy. Jom, 2021, 73, 4041-4050.	0.9	2
34	A Novel Microshear Geometry for Exploring the Influence of Void Swelling on the Mechanical Properties Induced by MeV Heavy Ion Irradiation. Materials, 2022, 15, 4253.	1.3	2
35	Evaluation of the Monte Carlo method (KTMAN-2) in fluoroscopic dosimetry and comparison with experiment. Journal of the Korean Physical Society, 2014, 64, 936-940.	0.3	1
36	Influence of Irradiation-Induced Defects on Anion Transport in Epitaxial Cr ₂ O ₃ . Microscopy and Microanalysis, 2021, 27, 2904-2905.	0.2	1

#	Article	IF	CITATIONS
37	Limitations of Thermal Stability Analysis via In-Situ TEM/Heating Experiments. Nanomaterials, 2021, 11, 2541.	1.9	0